

Coping with Information Extraction from In-Situ Data Acquired in Natural Streams

Özlem Baydaroglu¹, Marian Muste¹, Beyza Cikmaz^{1,2},
Kyeongdong Kim¹, Ehab Meselhe⁴ Ibrahim Demir^{1,3,5}

¹ IIHR – Hydrosience & Engineering, University of Iowa, Iowa City, Iowa, USA

² School of Urban and Regional Planning, University of Iowa, Iowa City, Iowa, USA

³ Dept. of Civil and Environmental Engineering, University of Iowa, Iowa City, Iowa, USA

⁴ Dept. of River-Coastal Science and Eng., Tulane University, New Orleans, LA, USA

⁵ Dept. of Electrical and Computer Engineering, University of Iowa, Iowa City, Iowa, USA

Abstract

Flood waves propagating in natural streams are highly complex flow situations with intricate dependencies among flow variables that are still not well understood. The most relevant information for deciphering these dependencies is extracted from continuous in-situ measurements acquired through high sampling frequency with special attention to the magnitude and timing of the hydrograph peaks. The new generation of acoustic instruments can produce experimental evidence if the useful nonlinear, nonstationary signals are extracted from the inherently noisy dataset acquired on site. This study presents a new screening protocol to smoothen streamflow data from the unwanted influences and noise generated by flow perturbations and observational fluctuations. The protocol is flexible and robust combining quantitative (statistical fitness parameters) and qualitative (domain expert judgments) evaluations. The screening protocol is tested with 18 smoothing methods applied to 118 datasets to identify the optimal data conditioning candidates. Sensitivity analyses are conducted to assess the validity, generality, and scalability of the smoothing procedures. The main goal of this analysis is to set a mathematical foundation for the empirical results that can lead to unified, general conclusions on principles or protocols for unsteady flows propagating in open channels, formulating practical guidance for future data acquisition and processing, and using the in-situ data to better support numerical and data-driven modeling efforts.

Keywords: river flow, data pre-processing, data smoothing, flood wave propagation, sensitivity analysis

This manuscript is an EarthArXiv preprint and has been submitted for possible publication in a peer-reviewed journal. Please note that this has not been peer-reviewed before and is currently undergoing peer review for the first time. Subsequent versions of this manuscript may have slightly different content.

1. Introduction

The main goal for the hydrologic and hydraulic data producer is to provide trustful in-situ datasets that accurately replicate the targeted process in their evolution over spatial-temporal scales. These data are subsequently used as reference for further understanding of the explored processes, validation, and verification of numerical simulations, as well as providing input datasets for data-driven simulations (Li and Demir, 2022) using canonical analytical methods or artificial intelligence (Findikakis & Savic, 2021, Krajewski et al., 2021; Sit et al., 2021). Using the much-needed experimental evidence for these purposes is typically challenging because the data are subject to perturbations inherent in natural environment and multiple uncertainty sources generated by the measurement process components. While perturbations are process- and site-dependent, hence somewhat preventable with proper caution, the sources of errors associated with measurement instruments, the execution of the measurement protocols and the setting of the parameters for data acquisition are unavoidable. In some instances, the acquired data points might not even illustrate the targeted processes. This is the case in situations where the measured variables are small with the data points embedded within the measurement noise or when sampling the flow with rates that are not sufficient to capture the frequencies of the flow fluctuations. Such situations are often encountered in the measurements for estimating the stream discharges whereby the flow variables vary widely in response to runoff inputs reaching the streams from highly variable and heterogenous landscapes (Mrokowska et al., 2013).

The immediate processes necessary in preparing the acquired experimental evidence for usage are data cleaning (for removing outliers) and data conditioning over time and space (used herein to broadly define procedures such as filtering, denoising, smoothing, interpolation (Baydaroglu and Demir, 2023), and extrapolation). These data pre-processing steps are critical for enabling the extraction of useful information from data (Muste et al., 2017). The cleaning and conditioning of the data are performed with a range of methods of varying levels of sophistication, with the most complex being those associated with the second category of data processing. The dominant methods for executing the two pre-processing tasks are statistical analyses solicited to attain context-specific information.

At a time of exponential growth of the data acquired in-situ due to the fast-paced advancement of highly productive digital instruments (e.g., non-intrusive acoustic probes for stage and velocity measurements), experimental investigators in hydrology and hydraulics are increasingly preoccupied to identify and optimize the methods for conditioning big data (Swarup et al., 2018, Runge et al., 2023; Demir and Szczepanek, 2017). The efforts for denoising the data are also required by the increased availability and usage of the new generation of field instruments that enable a dramatic increase of the temporal resolution of the measurements (often less than 1 measurement per minute). Similar trends in data processing are noted for modern instruments acquiring data over large scales with high spatial density. It can be asserted that the positive aspect of tracking processes with finer spatiotemporal granularity is partially counteracted by the burden of conditioning large amounts of data with increased level of noise.

The authors have come to the realization of the critical importance of data cleaning and conditioning when attempting to decipher the relations between flow variables in the propagation of unsteady flows through natural channels measured with high-resolution instruments (along the line of data-driven research initiated by Muste et al., 2022a). Of special importance for the present context is to capture the multivariate dependencies of the hydrographs around their peaks. These relationships, rarely investigated with prior in-situ measurements, are increasingly scrutinized (Muste et al., 2020, 2022b). Difficulties arise as the useful signals are contaminated by environmental factors present at the site (e.g., debris, waviness at the free surface, probe obstructions - Baydaroglu et al., 2018) as well from sensor-induced errors (e.g., probe accuracy, hardwired data processing, time drift, loss of calibration - Smith et al., 2010),

It appears that the authors' efforts to increase the level of confidence in the hydrometric data acquired in-situ with modern instrumentation are not isolated. Karlof et al. (2005) evaluate five techniques for detection of peaks in geophysical time series. Wang et al. (2019) applied filtering and several smoothing methods to continuous river surface velocity microwave radar data. Three smoothing methods were implemented and evaluated for obtaining discharge time series using the velocity-area method (Lique & Acosta, 2021). A notable effort is the work of Nazir et al. (2019) that developed a four-stage framework for addressing the noise complexity in multi-scale river flow time series that are intrinsically nonstationary as a process as well as noise characteristics. The above studies do not offer clear-cut recommendations on the efficiency of various types of pre-processing and smoothing methods. Instead, they provide comparisons of the results obtained with various smoothing methods and their sensitivity to the change in the smoothing parameters.

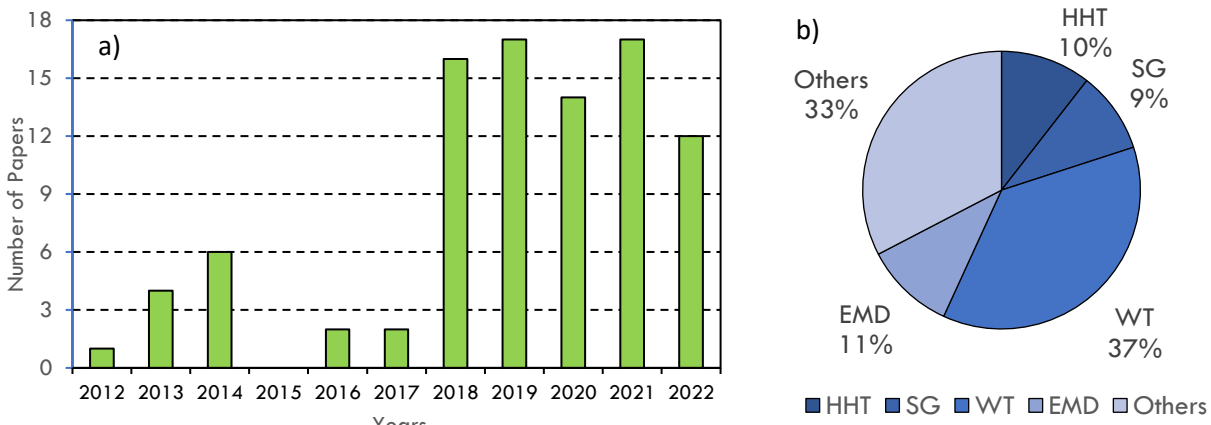


Figure 1. Summary of usage of de-noising methods in the 2012-2022 decade based on the review of 95 papers on the subject: a) increase of the number of papers on the subject; b) distribution of the de-noising methods in the reviewed studies.

A synthetic summary of the bibliographic evidence conducted by these authors indicates that the hydrologic and hydraulic community have increased their attention to the data cleaning problem, as illustrated in Figure 1a. The search for adequate methods for denoising the measurements become a burdensome task as there is a wide variety of methods that the users can

choose from (see Figure 1b). The frequency of usage of various methods suggests a quite leveled field, with Wavelet Transforms (WT) as the most popular method and Empirical Mode Decomposition (EMD), Hilbert-Huang Transform (HHT), and Savitzky-Golay Smoothing (SG) of balanced use. The fact that the “Others” category represents 33% of the used methods (including the Kalman Filter, Moving Average, Gaussian Filter, Variational Mode Decomposition, Friedmann’s Super Smoother) indicates that the smoothing algorithms are still in development.

Based on the literature purview, it can be reckoned that the choice of method used for cleaning the data is overwhelming with clear guidelines for users to decide. However, the apparent simple task of denoising the data is not trivial when approached with multiple pre-processing methods as each method provides a slightly different result and the true values of the measurements are not available for ground-truthing. The primary objective of this study is to ascertain optimal techniques for smoothing hydrologic and hydraulic data acquired with high sampling rates in unsteady flows propagating in natural rivers. Data pertaining to index velocity, stage, and free-surface slope acquired at several streamflow monitoring stations were utilized, along with the application of 18 distinct smoothing methods. To achieve the intended objectives, a sequential process for identifying the optimal smoothing technique was first developed to narrow the selection choices based on user-imposed criteria. Subsequently, sensitivity tests were carried out to assess the robustness of the smoothing algorithms to the data acquisition frequency and the signal-to-noise level of the raw data.

2. Data Context and Study Motivation

The context of this study revolves around the relevance of the raw data points acquired in situ with direct measurements of the variables used for continuous estimation of flow discharges in natural streams (streamflow) during steady and unsteady flows (Muste et al., 2020). The continuous monitoring of the streamflow in natural rivers cannot be made with direct discharge measurements even if the most advanced instruments, such as Acoustic-Doppler Current Profilers (ADCP), are used as the data acquisition is expensive and requires permanent operator presence at the site. Instead, indirect methods for estimation of discharge are used whereby unassisted measurements of flow variables are automatically and continuously recorded and subsequently used to estimate the discharge via rating curves (ratings) or flow governing equations.

The ratings are graphically constructed relationships based on trial-and-error protocols applied to large samples of direct discharge measurements simultaneously acquired with easier to measure variables such as stage (flow elevation), index-velocity (at a point, line, or surface) or free-surface slope. The rating construction can take more than one year to develop to include a sufficient number of data points covering uniformly the range of flows passing through the station. Once the ratings are established, discharge estimates (surrogates) are produced in real-time, typically at 15 minutes apart by entering in the rating the continuously measured variables (Demir et al., 2015).

The conventional rating-based methods used in the US are the stage-discharge (labelled as HQRC) and index-velocity method (labelled as IVRC). The first method uses a stage-discharge rating. The second method uses a rating relating stage to cross-sectional area and another one

relating the measured index-velocity with the cross-sectional mean velocity. These methods benefit from robust implementation protocols (Rantz, 1982 for HQRC and Levesque & Oberg, 2012 for IVRC). A third alternative for continuous monitoring is the Continuous Slope Area (CSA) method that is based on the energy conservation equation (Muste et al., 2019). The direct inputs for CSA method are the free-surface slope determined from stage measurements at (minimum) two locations and the cross-sectional geometrical characteristics obtained from a one-time geodetic survey. The ratings require continuous verifications to detect potential changes of the flow conditions at the site.

The capabilities of the three streamflow monitoring alternatives to measure steady and unsteady flow are extensively discussed in Muste et al. (2020). The focus of Muste et al. (2020) is on how well can monitoring methods capture the actual flows on the rising and falling stages of unsteady flows associated with the gradual propagation of the waves in the channel. Given that the channel flow is intrinsically different on the rising and falling stages of a wave propagation, the relationships among flow variables are affected by the so-called hysteresis visualized as a non-unique relationship in the dependence between two variables (Prowse, 1984).

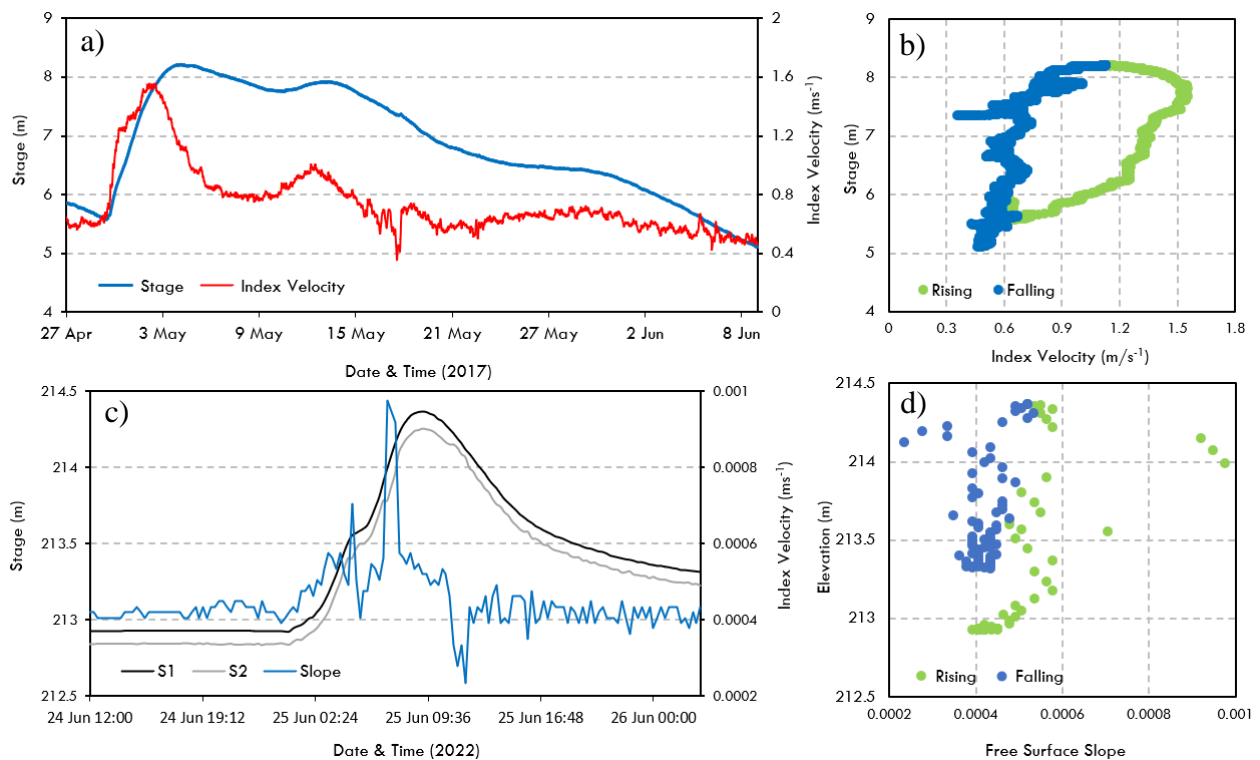


Figure 2. Time-dependent and time-independent relationships between raw data for the flow variables used for the estimation of discharge with the Index-velocity method (IVRC, Figures a, b) and Continuous Slope-Area method (CSA, Figures c, d) methods applied to unsteady flows: a) and c) time series of the measured flow variables displaying a phase shift; b) and d) loops in the relationships between the measured variables for the rising and falling limbs of the hydrographs.

The simple stage-discharge relationship does not capture the hysteresis at all as its construction is based on steady flow assumptions. Semi-empirical corrections are needed to substantiate the hysteresis (WMO, 2010). The addition of dynamic variables in the IVRC and HQRC methods allows to capture hysteresis with some degree of confidence, as illustrated in Figure 2. Hysteresis appears differently in time-dependent and time-independent plots, i.e., as shift among the hydrographs of the variables, and as a looped relationships between any of two of the flow variables, respectively (Muste et al., 2020). The magnitude of the loops and phase-lag between hydrographs are directly proportional to the slope of the channel at the site and magnitude of the events, with the lowest hysteresis presence being on steep rivers and small magnitude storm propagation events.

The capabilities of the IVRC and CSA methods equipped with new high-temporal resolution instruments (most of them based on acoustics principles) allow us to investigate basic river mechanics processes with a fresh perspective that was not possible to obtain with the data produced by the HQRC. The new datasets offered by the IVRC and CSA are not only ensuring more accurate flow measurements during steady and unsteady flows. These datasets can better support the interaction with numerical simulations and open a plethora of opportunities for data-driven investigations, including streamflow forecasting of the magnitude and the timing of the flood wave crest (Muste et al., 2022a). However, before embarking on the new possible dataset explorations, a necessary step is to clean the data by the unwanted flow perturbations and the noise from various sources associated with the measurements.

The raw data captured in Figures 2a and 2c illustrate that the IVRC and CSA method reveal the trends expected due to hysteresis presence (Muste et al., 2020). The data in these figures also reveal that natural flow perturbations and errors accumulated through the measurement process produce persistently “noisy” signals that obscure the details of the useful signal, especially around the signal peaks. The level of noise is not the same across variables with considerably lower levels for the measurement of stage compared to the raw index velocity measurements. One reason for the difference is that the stage varies over a larger range than the index velocity. Even for the smoother stage data points, the free-surface slope plot determined with such measurements is consistently noisy. One immediate explanation would be that the slope varies over the smallest range of all flow variables, and it is also of small magnitude.

In addition, the slope measurement is made at two locations, where the free-surface conditions at the two points can be exposed to different influences. Smith et al. (2010) note that an error of about 0.03 m in the fall of the free surface can lead to a discharge estimated with the CSA method that is off by about 25%. It should be noted that the smoothness of the time series plotted in Figure 2 is also affected by the time span used to visualize the series, with the latter being dictated by the duration of the flow event propagation. We limit our discussion herein to the primary flow variables, but the noise can be further amplified or dampened if the raw datasets are combined to obtain new flow variables (e.g., discharge).

The need for data smoothing varies with the purpose of the study which in our case is the accurate description of the peaks of the hydrographs. These peaks are essential in defining

analytical dependencies between the variables, with both the exact magnitude and timing of the peak being crucial for analysis. Also important are the gradients of the variables leading to the peaks and the overall shape of the hydrographs (see Muste et al., 2022a). Notably, each storm event propagating at a specific site is characterized by unique dependencies, hence the critical importance for accurate description of the hydrograph peaks in each newly analyzed dataset. Generalization of the knowledge on hysteresis relies heavily on in-situ observations as the complex causal relationships between the flow variables in unsteady open-channel flows are uncertain due to the complexity of the process (Hager et al., 2019). Some of the processes associated with hysteresis are scantily documented or not reported at all (e.g., the phasing of the hydrographs).

The hysteresis-related dependencies observed in natural streams are also affected by multiple intricacies generated by perturbations in the flow. Of special importance for the present study is the identification and accurate description of the local changes in the hydrographs generated by small changes in precipitation intensity or inflows from upstream tributaries entering the stream reach where the gaging is made. These perturbations appear as superposed “pulses” in the storm hydrographs, as illustrated in Figures 2a (on the falling limb) and 2c (on the rising limb). We define pulses as groups of consecutive data points on flow variable hydrographs reflecting a flow acceleration-deceleration cycle. Pending on the pulse magnitude, the local peak on one variable might result in a distinct peak or an inflexion point in the trend of the other variables (Muste et al., 2022a). The presence of the pulses complicates the interpretation of the overall flood wave characterization especially when they occur close to the flood crest (conventionally defined as the maximum value of the stage hydrograph for a given storm).

The short description provided above is sufficient to make the case that the inherent noisiness and perturbations of the signals used for estimation of the flow discharge can hamper the attempts to parameterize and generalize the signature of hysteresis with the level of detail required for a ground-truth dataset. Consequently, robust protocols for data conditioning and their thorough evaluation are required for the advancement of this emerging research. The smoothing protocols have to preserve the nonlinear and nonstationary nature of the flow propagation processes as the theoretical or numerical predictions are of limited reliability or not available at all. Finally, we should mention that in the present analysis we assume that the available sampling frequency (1 measurement/15 minutes) is sufficient to capture accurately the peak hydrographs even during fast-evolving (flashy) events. A discussion on the impact on the smoothing is provided using a frequency of sampling of 1 measurement/1 hour) to illustrate this effect.

3. Smoothing Algorithm Selection

3.1. Smoothing Procedures and Dataset

The process of extracting useful data from the raw measurements can be approached using several methods, such as filtering, smoothing, and decomposing the signals. These methods aim to minimize noise in accordance with specific research objectives. The process of noise reduction first involves the elimination of the signal's extreme values that might result in a reduction of the signal's average magnitude (Kowalski & Smyk, 2018). Noise reduction algorithms subsequently

applied can be divided into two groups: filtering and smoothing. Filtering imposes constraints on a time-dependent variable applied at the most recent measurement time (t). Smoothing imposes constraints over specific time intervals, time spans preceding and following time (t) instance. Table 1 summarizes the set of 18 smoothing techniques employed in the present analysis.

Table 1. The smoothing algorithms tested in this study.

Methods	Description
3-point, 5-point, 7-point, 9-point Moving Average (MA), 3-point Weighted MA (3pWMA), 3-point Exponential MA (3pEMA)	The MA mitigates temporal fluctuations in time series data by computing the mean of neighboring values (p) within symmetrically selected points in the time series (Maity, 2018).
Exponential Smoothing (ES)	ES employs an exponentially decaying weighting function of past observations in a time series (Hannachi, 2021).
Linear Regression (LR)	LR represents the relationship between two variables by fitting a linear equation to data.
Quadratic Regression (QR)	QR is an extension of linear regression for a data set with a parabolic form.
Gaussian Smoothing (GS)	GS calculates the gradient by randomly sampling parameters from the standard normal distribution and performing finite differences as an optimization technique (Gao and Sener, 2022)
Locally Weighted Scatterplot Smoothing (LOWESS)	LOWESS is a non-parametric approach for fitting multiple regression analysis in the local area (Cleveland, 1979; Cleveland and Devlin, 1988).
Kernel Smoothing (KS)	KS, which is a commonly used nonparametric method, is a type of weighted moving average (Nadaraya, 1964; Watson, 1964).
Empirical Mode Decomposition (EMD)	Using EMD, a nonstationary signal is empirically decomposed into a small number of sub signals that are thought to be locally stationary (Huang et al., 1998).
Discrete Wavelet Transform (DWT)	DWT is a linear operation that decomposes a given signal into a number of sets consisting of a time series of coefficients as indicators of the signal's temporal evolution in the frequency band (Daubechies, 1988; Mallat, 1989).
Friedmann's Super Smoother (FSS)	FSS is a nonparametric regression estimator with adaptive bandwidths that is based on local linear regression (Friedman, 1984).
Savitzky-Golay Smoothing (SG)	By piecemeal fitting a polynomial function to the signal, the SG filter smooths a noisy signa (Savitzky and Golay, 1964).
Hilbert-Huang Transform (HHT)	HHT is a two-stage method that begins with adaptive data decomposition into intrinsic mode functions and then proceeds

	to Hilbert spectral analysis to construct an energy-frequency-time distribution (Huang et al., 1996, 1998, 1999).
Whittaker-Henderson Smoothing (WHS)	WHS is a discrete-time spline smoothing for identically spaced data (Whittaker, 1922, 1925; Henderson, 1924, 1925).

The screening of the smoothing algorithms is presented in conjunction with time series of the raw (as sampled) index-velocity data acquired every 15 mins at a USGS gaging station on Henry River in Illinois (USGS # 05558300) for the year of 2015. The station, located on the Illinois River, is 200-m wide on a 0.0002 bed slope reach. A dataset of 6 years recorded at this station was analyzed to characterize the hysteretic behavior across storm events (Muste et al., 2022b). The year 2015 was selected for the present analysis to facilitate the simultaneous analysis of multiple smoothing procedures and as it contains the largest storm in the 6-year records. This series is illustrated in Figure 3. The 2015 data sample selected for testing entails ten major storms illustrated by dashed line rectangles in Figure 3. The candidate smoothing algorithms were applied to the 15-min as reported in Section 3.2. The 1-hr datasets, derived from the 15-min data are discussed in Section 4.2.

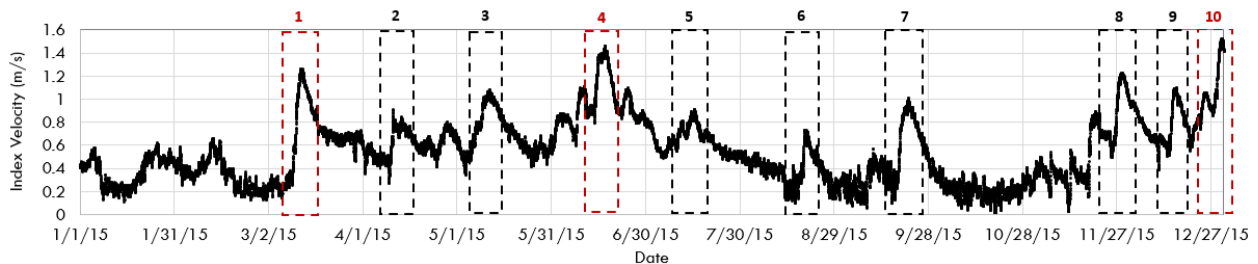


Figure 3. Time series of 15-min index-velocities recorded in 2015 at the USGS gaging station #05558300.

3.2. Evaluation of the Optimal Smoothing Procedures

Given that the main goal of screening is to evaluate the performance of the algorithms around the absolute peak of each storm hydrograph, we developed a four-step phased screening protocol for algorithm selection as schematically illustrated by the central block (yellow color) of the flowchart in Figure 4. The evaluation criteria for assessing the smoothing quality entails the difference in the peak magnitude, and the time of peak occurrence. The first three steps of the screening are quantitative. The fourth step is a combination of quantitative and qualitative assessments with the latter based on visual inspection of the shape of the smoothed datasets compared with trends in the raw signal. The visual inspection relies on domain expert knowledge that is aimed to fill the gaps left by the purely quantitative evaluation.

In the first step of the screening process, the differences between the raw and the smoothed datasets for multiple storms. The differences are quantified by magnitude of the average error percentages between absolute values in the raw data series and the continuous trend line produced by smoothing protocols for the time instances when raw data was sampled. Methods exhibiting

average differences of 10% or greater are excluded from the subsequent analysis. During the second screening step, the mean absolute percentage error (MAPE) is computed using the raw and the smoothed datasets preserved after the first screening step. Datasets with MAPE values exceeding 10 are removed. In the third step of the screening, the evaluation of the smoothing methods is made based on magnitude of the peak shifts between the smoothed and observed time series. The protocols that displayed time shifts larger than 20 data points (equivalent to 5 hours in the 15-min records) are eliminated.

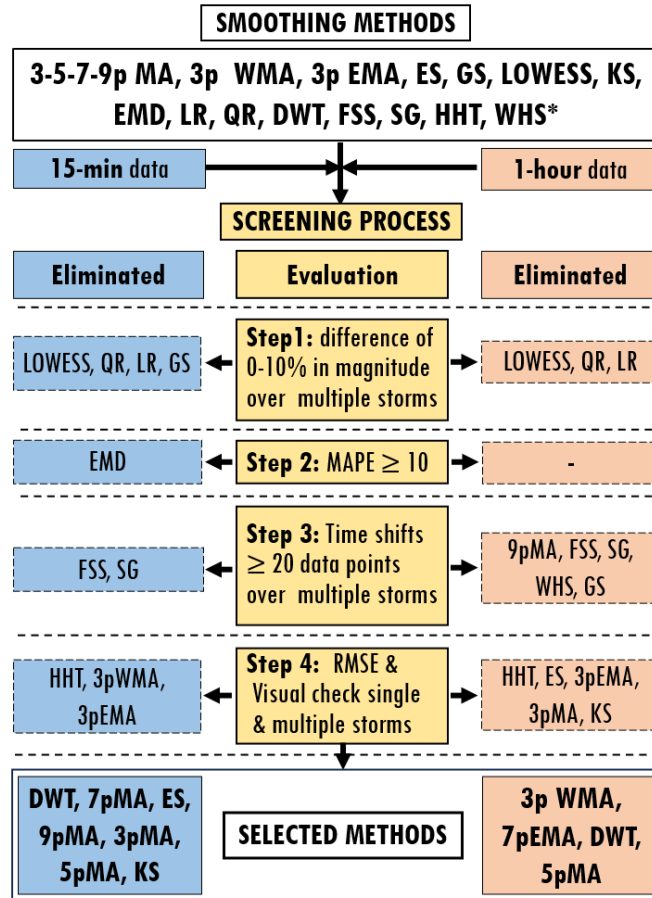


Figure 4. The flow of a sequential process for screening the optimal smoothing techniques for the index velocity time series recorded in 2015 at USGS# 0555830 gaging station. * WHS could be only applied for smaller size datasets.

Step 4 of the smoothing procedure screening is predicated by the evaluation of the root mean square errors (RMSE) value (quantitative criteria) in conjunction with visual inspections (qualitative criteria). The role of the visual inspections is to compare the smoothen data trace with the expected trends predicted by expert knowledge on the hysteretic behavior. An ad-hoc set of user-driven criteria is assembled for this purpose to determine allowable shifts in magnitude and time around what is perceived to be the overall peak for individual storms. The visual criteria are subjective as they depend on the users' skills and familiarity with the hysteresis process associated

with unsteady open-channel flow. The judgement of the visual appearance is complicated by the presence of multiple local smaller peaks in the vicinity of the overall flood wave peaks for individual storms (starting and ending close to the base flow for the site). The multi-peak feature is not expected to be induced by noise. Rather, it might be attributed to the fluctuations of the flows that are inherent in natural scale open channel flows. The shifts in the datasets can, almost certainly, be attributed to the effect of the smoothing method that is directly dependent on the smoothing window selected around the overall peak.

In this section, we describe the step-by-step implementation of the screening procedures for determining the optimal smoothing approaches along with the evaluation of the screening results as applied to the targeted raw 15-min index-velocity dataset. A total of 118 datasets were generated by employing various smoothing techniques, with each technique being applied using distinct smoothing parameters and spans. The numerical and graphical evaluations were executed with the programming language R and MATLAB analysis platform. The blue boxes are tracking the smoothing procedure performance for the 15-min index-velocity data, while the orange boxes are relevant for the 1-hr dataset. The WHS method was only applied to the 1-hr data as for processing the whole year of 15-min data this procedure produces large size data that requires high-performance computing, that was not available for the present study.

The implementation of the joint quantitative-qualitative procedure assessment described in Figure 4 to the 15-min index-velocity data for the whole 2015 year led to the elimination of (see left side of Figure 4): LOWESS, GS, QR, and LR (in step 1), EMD (in step 2), FSS and SG (in step 3), and HHT, 3p WMA, and 3p EMA (in step 4). Table 2 displays the numerical values for the quantitative and visual performance of the best seven smoothing techniques tested for the whole 2015 year of the 15-min index-velocity data acquired at USGS gaging station # 05558300. Except for the 3-5-7-9p MA methods, all the other smoothing approaches were selected following a careful evaluation of the processing parameters (i.e., smoothing spans, weights, functions, and wavelet types for DWT method). These parameters vary depending on the data type and sampling rates. Only combinations that yielded optimal outcomes are presented below.

Table 2. The optimal statistical methods for analyzing raw 15-min index velocity dataset for the major storms of the year 2015.

Method	RMSE	MAPE	% Difference in peak magnitude (10 storms)	Time shifts in the peaks (10 storms)	Visual check passes (10 storms)
DWT	0.005	0.923	0.544	5	10
7p MA	0.007	1.358	1.179	8	6
9p MA	0.009	1.724	1.531	12	5
3p MA	0.004	0.734	0.565	4	4
5p MA	0.005	1.049	0.857	8	4
KS	0.004	0.735	0.531	11	4
ES	0.012	2.468	2.233	12	7

An inspection of the numerical values presented in Table 2 substantiates that DWT emerges as the most effective method based on its better performance in terms of error magnitudes, temporal shifts, and visual inspections of the trend lines for the smoothed and raw data. Moreover, it can be observed that while the ES technique meets the criteria for most visual assessments, it exhibits inferior performance in terms of error magnitudes and temporal shifts when compared to the other six approaches.

While the screening results are available for all ten major storms, here we illustrate the visual evaluation of the smoothing algorithms for three storms in the year 2015 (i.e., first, fourth, and tenth) as they are the largest in the dataset and feature complex variation around their peak. Using the Savitsky-Golay (1964) approach for characterizing the peak-to-base ratio (i.e., the fraction of a storm peak value from that of the largest storm), the respective ratios are 0.82, 0.96 and 1.00 for these peaks. Figures 5–7 depict graphs and heat maps illustrating the index-velocity raw data smoothed with the seven best methods for storms 1, 4, and 10 in 2015. The graphs were generated based on a set of 20 neighboring data points located in the proximity of the overall peak for each individual storm. The heat maps were calculated using all the storms of the 2015 year. Temporal alterations are readily observable inside the maps by the patterns in the central green area of the heat maps. The peak values for each approach are indicated by bold letters in these maps.

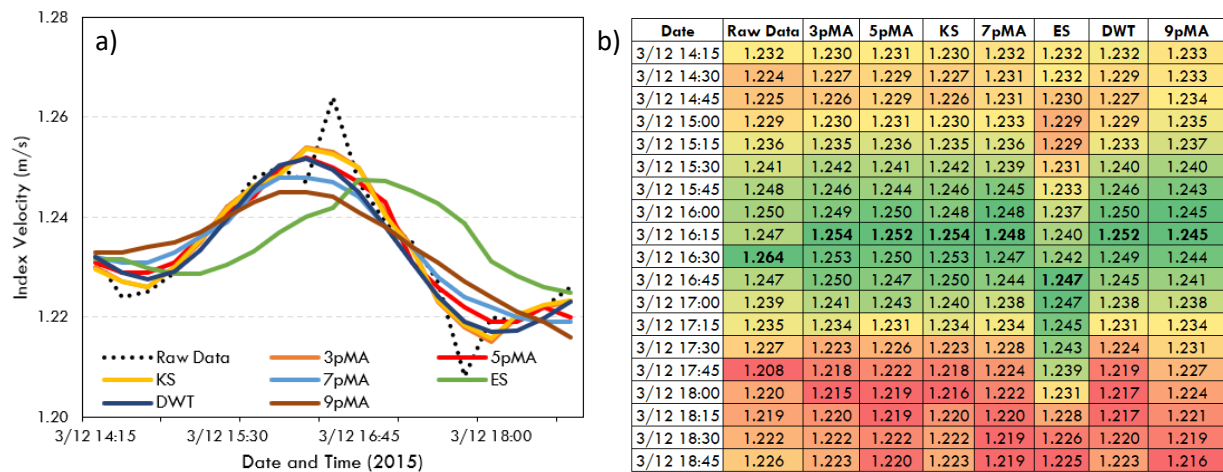


Figure 5. Smoothed data obtained with the optimal methods applied to the 15-min index-velocity data of the 1st storm of 2015: (a) smoothed index velocity data, (b) the heat map of the smoothed datasets.

These graphical representations in these figures indicate that the optimal smoothing methods are bundled in an overall trend for the individual storms. An exception is the ES method that is visibly shifted in magnitude and timing for all the three individual storms, which is consistent with the numerical evaluations provided in Table 2. The examination of the individual storm events in Figures 5-7 indicates that using the 3-5p MA methods exhibit several peaks around the wave crest. This feature is gradually weakening for the 7-9p MA methods with the preservation of the trends indicated by the raw data. Similarly, the DWT, GS, LR, KS, FSS, QR, and SG fail to identify local

peaks around the overall storm peaks as also somewhat indicated by the numerical values of RMS, MAPE, and percentage magnitude difference listed in Table 2. In order to complete the evaluation analysis, we present the performance of the eliminated methods for the 15-min data of the fourth storm of 2015 (see Figure 8). The graphs in this figure illustrate that, excepting the 3pWMA method, all the sub-optimal smoothing ones are performing poorly based on Step 4 of the screening protocol.

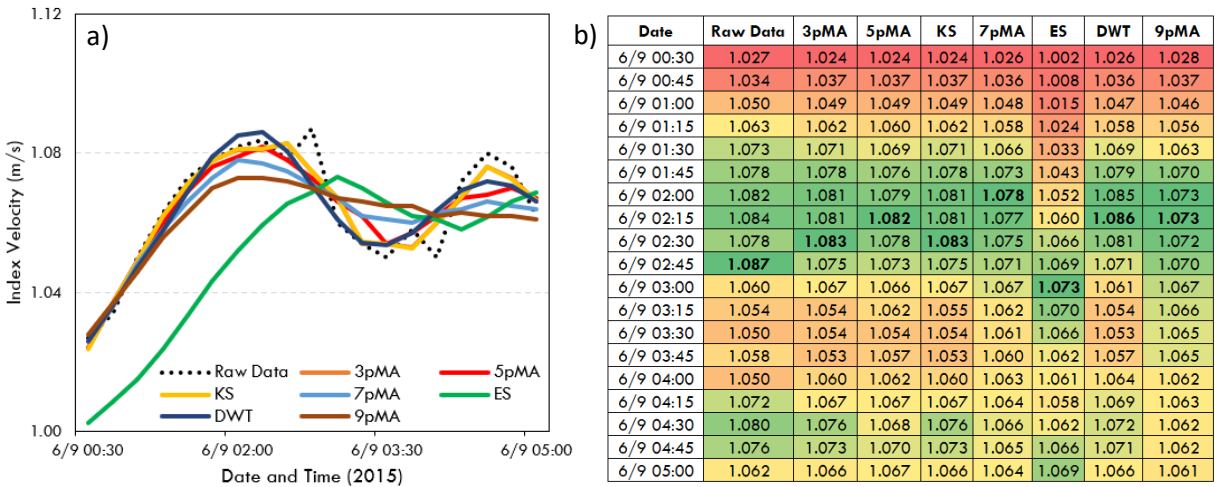


Figure 6. Smoothed data obtained with the optimal methods applied to the 15-min index-velocity data of the 4th storm of 2015: (a) smoothed index velocity data, (b) the heat map of the smoothed datasets.

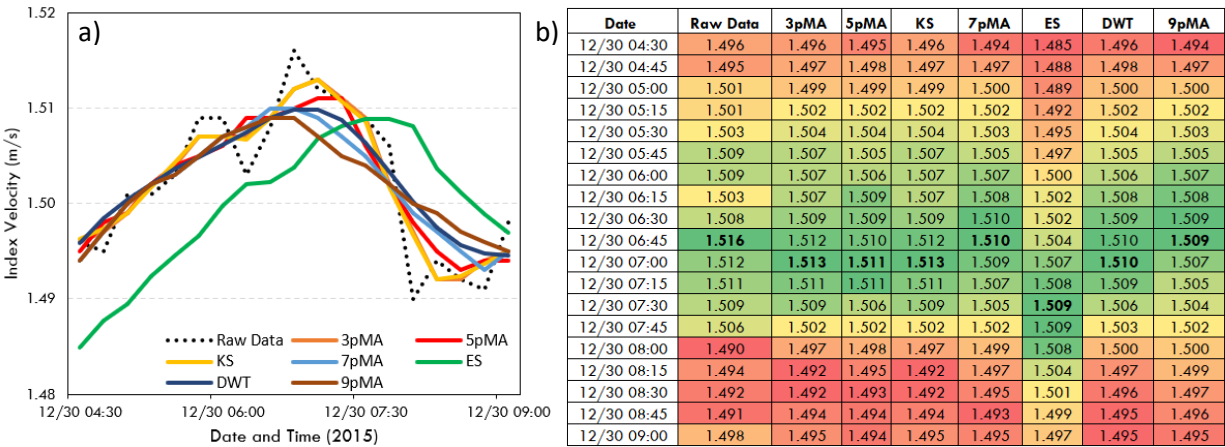


Figure 7. Smoothed data obtained with the optimal methods applied to the 15 min index-velocity data of the 10th storm of 2015: (a) smoothed index velocity data, (b) the heat map of the smoothed datasets.

4. Sensitivity Analysis

The sensitivity analysis aims at illustrating the impact of various data collection or processing parameters on the evaluation results reported above and extend the analysis for other sites and flow

variables tracking unsteady flows. For this purpose, we present the implementation of the smoothing procedures for flow variables used for discharge estimation with the IVRC and CSA methods. The case studies include datasets of stages and index-velocities acquired at several gaging stations and free-surface slope measurements derived from stages measured at two locations in the stream. We intentionally included a variety of river sizes as the hydrologic and hydraulic processes occurring in streams are developing at various temporal scales. The sampling rates used for acquiring individual variables are typical for those used at conventional gaging stations, i.e., about one reading every 15 minutes.

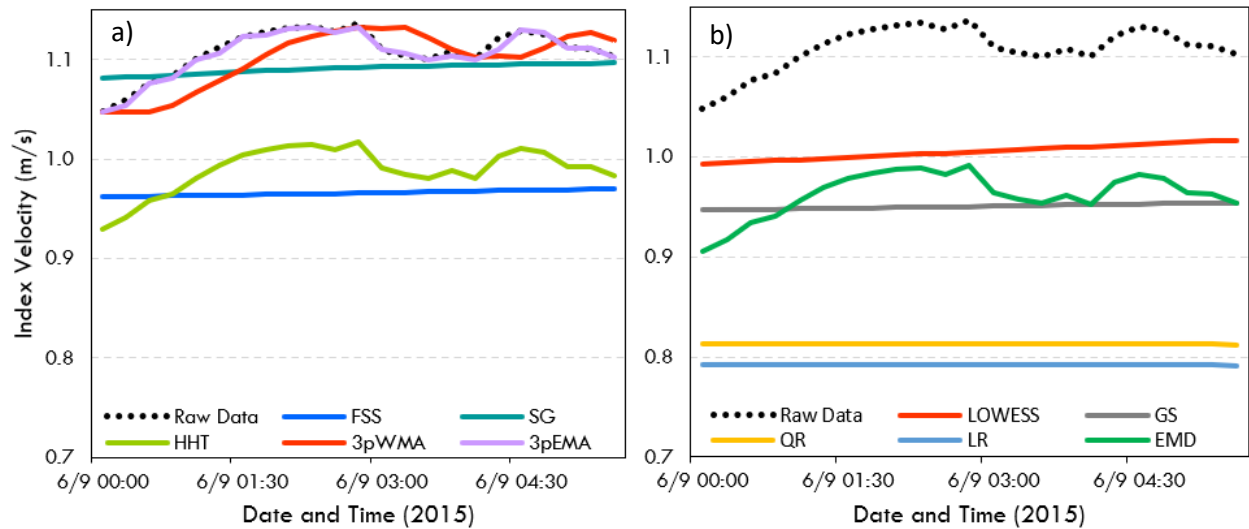


Figure 8. Traces of the smoothing methods eliminated in the screening phase of the analysis for the 4th storm peak of 15-min index-velocity data acquired at USGS gaging station #05558300: (a) smoothed data using FSS, SG, HHT, 3pWMA, and 3pEMA b) smoothed data using LOWESS, GS, QR, LR, and EMD.

4.1. Time Span for Smoothed Data Series

The analysis in Section 3 is based on the 15-min index velocity data points acquired during 2015 at the USGS gaging station 05558300. A question is posed regarding the performance of the selected smoothing approaches if they are evaluated for individual storms considered in isolation from the annual time series. The time spans for the individual events are illustrated by the rectangles in Figure 3. For this purpose, we compare the graphs of the optimal smoothing methods evaluated with the year-long and individual storm time spans using the 1st storm of the year 2015 for illustration. The shorter time span of the dataset for individual storms enables us to include in the evaluation the WHS smoothing method that could not be applied for the whole year time series because of computational limitations. Figures 9 show this comparison whereby plots tagged with “s” labels the smoothing method applied to a local time span around the peak of the first storm of 2015. The plots in Figure 9 demonstrate that the 3-5-7-9p MA methods yielded consistent agreement regardless of whether the entire year's data or the storms' data are used. It is also apparent that KS, ES and DWT reveal quite different dataset patterns. Notable is the high level of

effectiveness for the WHS applied to the time span of an individual storm, as can be seen in Figure 9 (h).

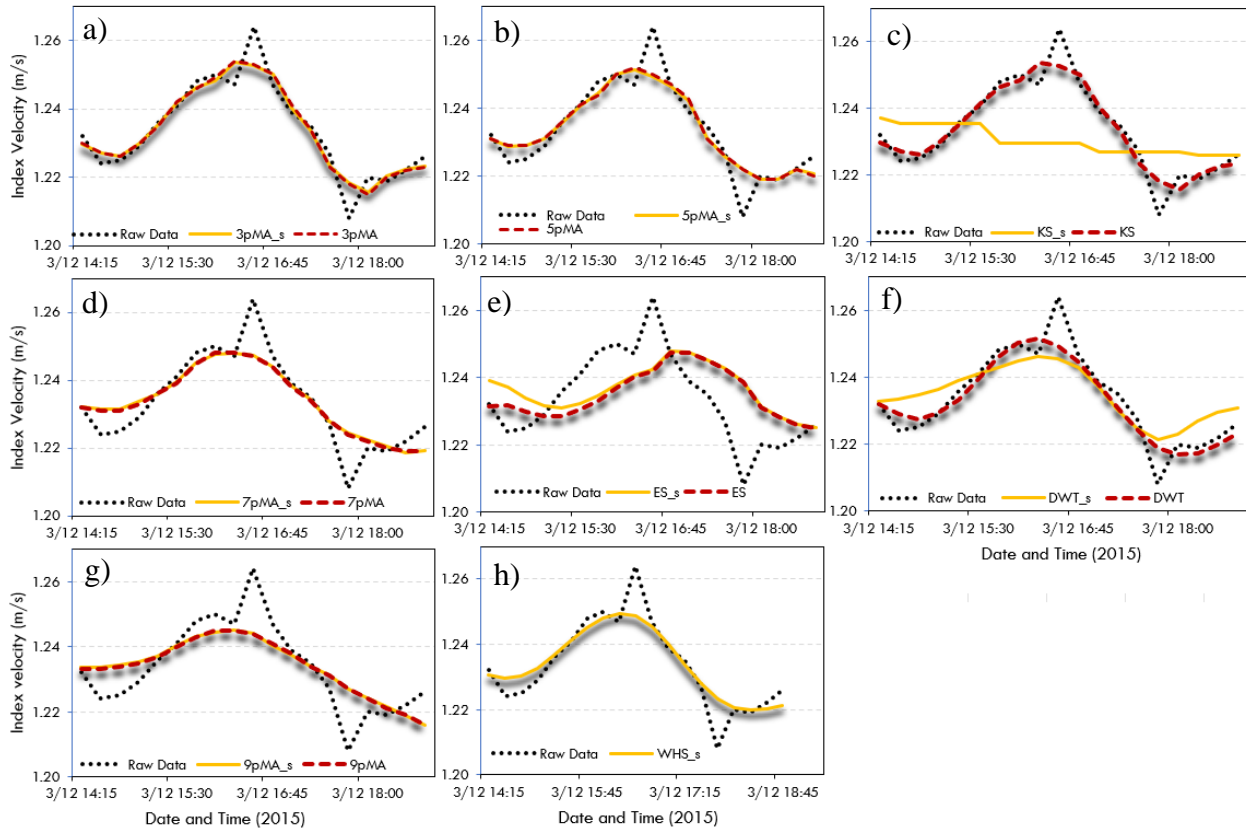


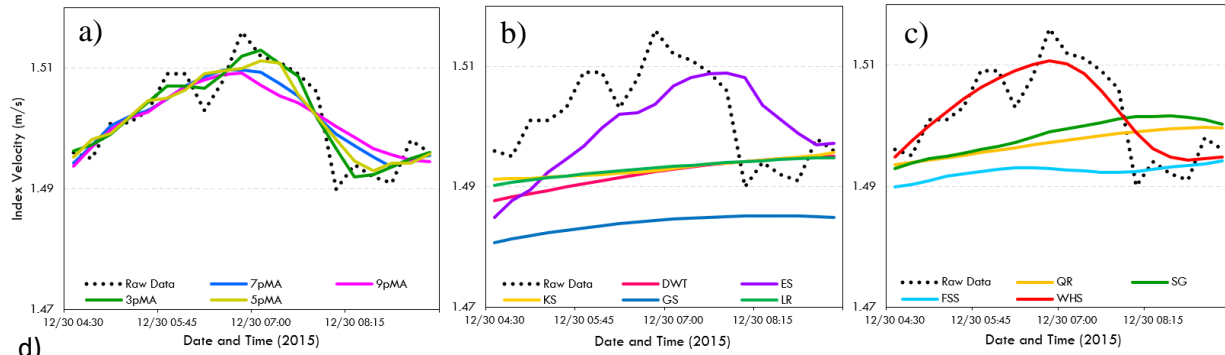
Figure 9. Implementation of the optimal smoothing procedures with year-long and event-long time span for the 1st storm in the 2015 time series of 15-min index velocity at USGS gaging station 05558300: (a) 3p MA (b) 5p MA (c) KS (d) 7p MA (e) ES (f) DWT (g) 9p MA (h) WHS.

A complete screening process, including the numerical and visual evaluation aspects, is provided for all optimal (i.e., DWT, 3-, 5-, 7, 9-p MA, KS and ES) along with a subset of the sub-optimal procedures (i.e., LOWESS, GS, QR, LR, EMD, and FSS) applied to the 15-min index-velocity data of the 10th storm (the largest of the 2015) passing through the USGS gaging station #055583000. Figure 10 illustrates the numerical and visual results of the raw data smoothening using the above-mentioned methods. The inferences on the quality of the smoothing for optimal and suboptimal methods from this test are quite similar with the ones reported above in this section, i.e., the 3-5-7-9p MA methods yielded consistently better agreements than the KS, ES and DWT methods. One can observe that the performance of the WHS method is in good agreement with the expected trends based on expert knowledge on the flow behavior during flood wave propagation.

4.2. Sampling Frequency for Acquiring Raw Data

The screening procedure was also implemented to the 1-hr data time series for the index-velocity data acquired for the 10 major storms of the 2015 year recorded at the USGS gaging station 05558300. This data was obtained from the 15-min index-velocity dataset illustrated in Figure 3

by uniformly discarding 3 consecutive points starting with the initial point in the 2015 time series. The process for determining the optimal smoothing technique utilizing hourly data followed the screening approach described in the yellow boxes of Figure 4. The successive elimination of the methods is shown in the orange boxes on the right side of the figure. The LOWESS, QR, and LR smoothing techniques were discarded during the first screening step. No methods were eliminated in step 2. The 9p MA, FSS, SG, WHS, and GS were eliminated during the 3rd screening step due to peak shifts exceeding 20 data points (equivalent to 20 hours). Finally, in the fourth screening step, the HHT, ES, 3pEMA, and KS were also eliminated.



d)

Date & Time	Raw Data	DWT	7pMA	ES	9pMA	3pMA	5pMA	KS	GS	LR	QR	SG	FSS	WHS
12/30 04:30	1.496	1.488	1.494	1.485	1.494	1.496	1.495	1.491	1.481	1.490	1.494	1.493	1.490	1.495
12/30 04:45	1.495	1.488	1.497	1.488	1.497	1.497	1.498	1.491	1.481	1.491	1.494	1.494	1.490	1.497
12/30 05:00	1.501	1.489	1.500	1.489	1.500	1.499	1.499	1.491	1.482	1.491	1.494	1.495	1.491	1.500
12/30 05:15	1.501	1.489	1.502	1.492	1.502	1.502	1.502	1.492	1.482	1.491	1.495	1.495	1.492	1.502
12/30 05:30	1.503	1.490	1.503	1.495	1.503	1.504	1.505	1.492	1.483	1.492	1.495	1.495	1.492	1.504
12/30 05:45	1.509	1.490	1.505	1.497	1.505	1.507	1.505	1.492	1.483	1.492	1.496	1.496	1.492	1.506
12/30 06:00	1.509	1.491	1.507	1.500	1.507	1.507	1.506	1.492	1.484	1.492	1.496	1.497	1.493	1.508
12/30 06:15	1.503	1.492	1.509	1.502	1.508	1.507	1.509	1.492	1.484	1.493	1.496	1.497	1.493	1.509
12/30 06:30	1.508	1.492	1.510	1.502	1.509	1.509	1.510	1.492	1.484	1.493	1.497	1.498	1.493	1.510
12/30 06:45	1.516	1.492	1.510	1.504	1.509	1.512	1.510	1.493	1.484	1.493	1.497	1.499	1.493	1.511
12/30 07:00	1.512	1.493	1.509	1.507	1.507	1.513	1.511	1.493	1.485	1.493	1.498	1.499	1.493	1.510
12/30 07:15	1.511	1.493	1.507	1.508	1.505	1.511	1.511	1.493	1.485	1.494	1.498	1.500	1.493	1.509
12/30 07:30	1.509	1.494	1.505	1.509	1.504	1.509	1.506	1.494	1.485	1.494	1.498	1.500	1.492	1.506
12/30 07:45	1.506	1.494	1.502	1.509	1.502	1.502	1.502	1.494	1.485	1.494	1.499	1.501	1.492	1.502
12/30 08:00	1.490	1.494	1.499	1.508	1.500	1.497	1.498	1.494	1.485	1.494	1.499	1.501	1.492	1.499
12/30 08:15	1.494	1.494	1.497	1.504	1.499	1.492	1.495	1.494	1.485	1.494	1.499	1.501	1.493	1.496
12/30 08:30	1.492	1.495	1.495	1.501	1.497	1.492	1.493	1.495	1.485	1.494	1.499	1.502	1.493	1.495
12/30 08:45	1.491	1.495	1.494	1.499	1.496	1.494	1.494	1.495	1.485	1.495	1.500	1.501	1.493	1.494
12/30 09:00	1.498	1.495	1.495	1.497	1.495	1.495	1.494	1.495	1.485	1.495	1.500	1.501	1.494	1.495
12/30 09:15	1.496	1.495	1.496	1.497	1.495	1.496	1.496	1.496	1.485	1.495	1.500	1.500	1.494	1.495

Figure 10. Smoothed data obtained with all optimal and a set of sub-optimal methods applied to the 15 min index-velocity data of the 10th storm of 2015 at the USGS station 05558300: (a) 3-5-7-9p MA (b) DWT, ES, KS, GS, and LR (c) QR, SG, FSS, and WHS; d) the heat map of the smoothed datasets (peak values estimated by each method are indicated in bold).

Table 3 presents the six most effective techniques for the smoothing of 1-hr raw index velocity data. It is apparent that the best methods display error magnitudes close to each other, while the

time shifts vary widely. Our screening process prioritizes visual inspections. Similar to the 15-minute index-velocity data at this station, the DWT and KS algorithms successfully pass the numerical aspects of the screening process. Figures 11-13 present the graphs for the visual evaluation of the best six methods applied to storms 1, 4, and 10 of 2015. The trends of the DWT and 3pWMA in Figures 10-11 indicate that these methods are marginally efficiency in matching the expected trends hinted by the raw data. In Figure 12, however, the 3pWMA method demonstrates better agreement with the expected trends.

Table 3. The optimal smoothing methods for the 1-hr index velocity dataset.

Methods	RMSE	MAPE	% Difference in peak magnitude (10 storms)	Time shifts in the peaks (10 storms)	Visual check passes (10 storms)
7pMA	0.019	3.779	3.569	18	8
DWT	0.026	5.584	2.571	20	6
3p WMA	0.022	4.586	3.244	14	5
5p MA	0.015	3.132	2.704	15	4
3p MA	0.011	2.197	1.346	3	3
KS	0.011	2.196	1.350	4	3

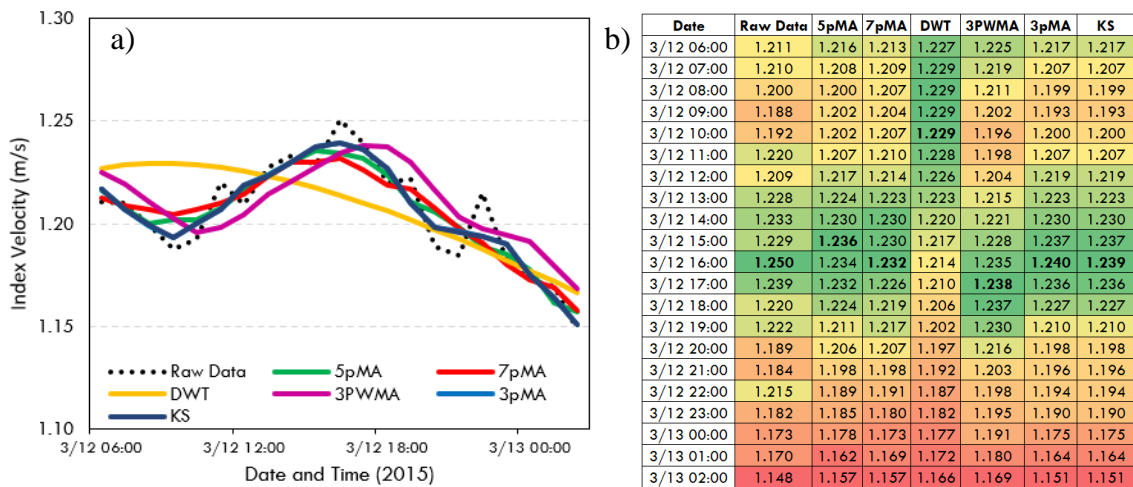


Figure 11. Smoothed data obtained with the optimal methods applied to 1-hr index-velocity data of the first storm of 2015: (a) smoothed index velocity data, (b) the heat map of the smoothed datasets.

The comparison of the optimal smoothing procedures applied to the 15-minute data (see Figures 5-7) with those applied to the 1-hr data (see Figures 11-13) reflects the relative larger spread of the obtained trends for the lower sampling frequency used in the measurements. Based on the evaluation results shown in Figures 11-13, it appears that the most appropriate smoothing technique for 1-hr data is the 7pMA. Similar with the analysis for the 15-min data at this gaging station, it is evident that MA-based methods hold a prominent position in the list of superior methods. Notably, the use of KS replicates relatively well the trends in the data. DWT, however,

produces good results only on the 15-minute data. The present and the above discussions illustrate the laborious effort and the challenge faced by users in selecting a unique optimum smoothing procedure.

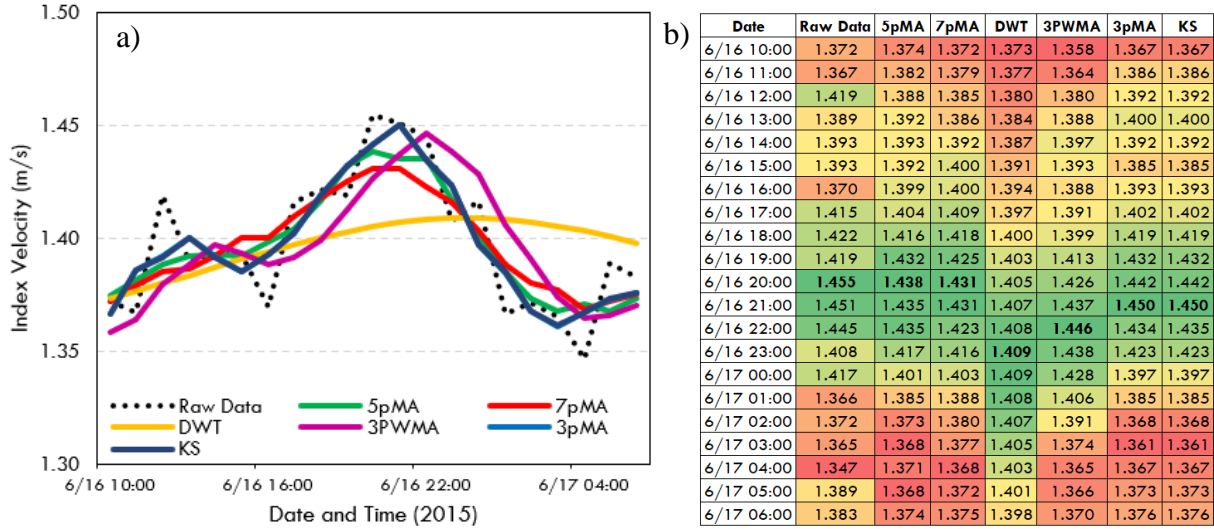


Figure 12. Smoothed data obtained with the optimal methods applied to the 1-hr index-velocity data of the fourth storm of 2015: (a) smoothed index velocity data, (b) the heat map of the smoothed datasets.

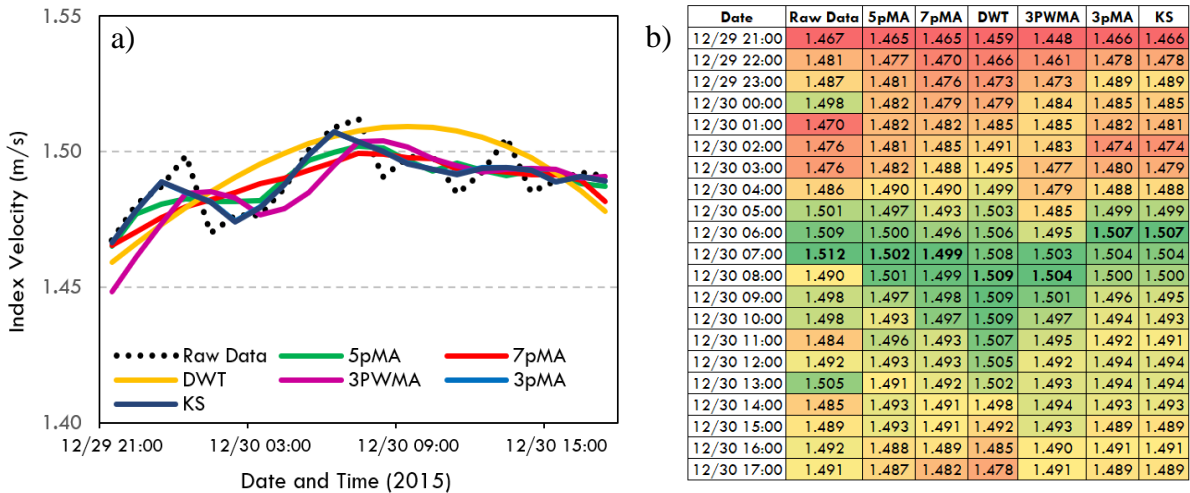


Figure 13. Smoothed data obtained with the optimal methods applied to 1-hr index-velocity data of the tenth storm of 2015: (a) smoothed index velocity data, (b) the heat map of the smoothed datasets.

4.3. Influences of Measurement Site and Data Acquisition Protocol

The data presented in this section was acquired with IVRC (the same monitoring protocol as in section 4.2 (i.e., IVRC) in the Yeongsang River (South Korea) at the gaging station 5004550 located near Naju Bridge. At this location, the river is about 150-m wide (at based flow) and has a bed slope of 0.00025. The sampling rate for the index-velocity data is 10-min that should benefit

the implementation of the smoothing protocols for data less frequently sampled (above 15 minute). The performance evaluation was made with the top seven methods identified as optimal in the analysis of the index-velocity data presented in section 4.1: DWT, 7-p MA, 9-p MA, 3-p MA, 5p-MA, KS, and ES). The other six methods eliminated in the screening protocol presented in Section 3 (i.e., LOWESS, GS, QR, LR, EMD, FSS, and DWT) of this study are also applied to this dataset for completion of the illustration and for checking the generality and scalability of the procedures. The numerical evaluations were made on the largest storm in 2020.

The evaluation results obtained with the 13 procedures applied for the selected storm are presented in Figure 14. The visual inspection of the trend lines in this figure suggests that the 3-p MA approach, KS and WHS follow closely the trends indicated by the raw data. The outcomes of the smoothing with the KS and DWT method are also found acceptable. Out of the optimal method set, the WHS is performing best. The least performant methods are the GS, LR, QR, and FSS approaches that fail altogether and the ES and SG approaches that show significant magnitude and time shifts compared with the raw data trends.

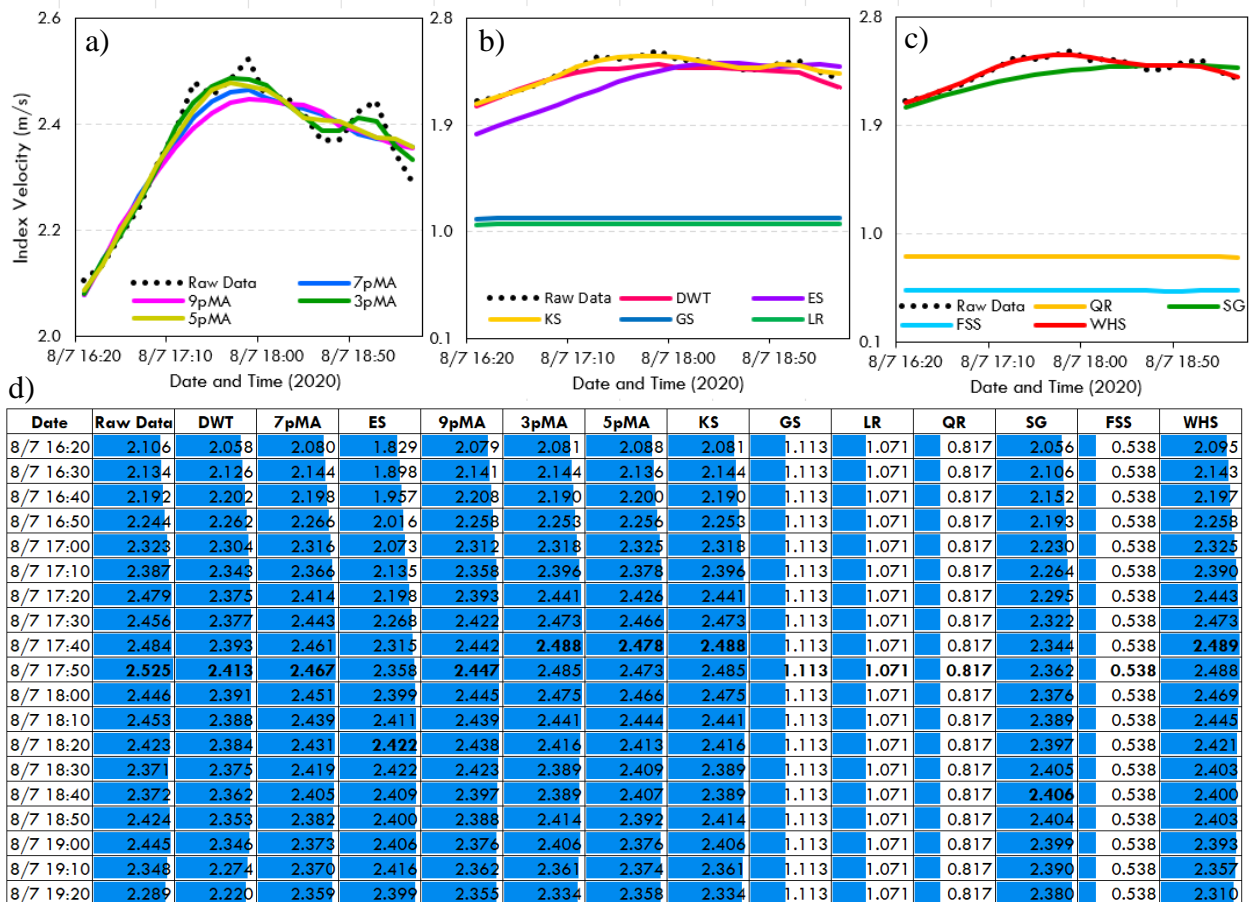


Figure 14. Smoothed data obtained with the selected methods applied to 10-min index-velocity data for a storm event at the Naju Bridge gaging site (Korea): a) smoothed data with 3-5-7-9p MA; b) smoothed data with DWT, ES, KS, GS, and LR; c) QR, SG, FSS, and WHS; and d) the heat

map of the smoothed datasets for 2020 (peak values determined by each smoothing procedures are printed in bold).

The present approach is grounded on the examination of a storm event. To provide an overview of the utilization of various methodologies on distinct datasets, the present study employed the top seven methodologies derived from an analysis of 15-min data. Also, six additional methodologies, which were commonly employed in the literature or excluded despite their relatively low error values, were also considered. For example, in terms of error values, the FSS and SG approaches had very good results. Nevertheless, within the datasets produced using FSS by changing smoothing parameters, the time shifts of the datasets that were not eliminated during the initial and subsequent screening phases exhibited a range of 69 to 82 (during the third screening, datasets with temporal shifts beyond 20 were excluded). The time shift for SG was between 28 and 82. Given the significant time shifts observed despite the relatively low error values, we incorporated these techniques into the six models to evaluate their performance on diverse data sets.

4.4. Measurement of Free-Surface Slope

The type of flow perturbations and noise in the acquired data are directly related to the measurement site, physical nature and range of variation of the measured variable and the type of instrument used for the measurements. Consequently, it is expected that the selection of the optimal smoothing procedures is dependent on all the above factors. In order to test this hypothesis, we implemented the 13 noise reduction procedures for smoothing index-velocity data to measurements of free-surface slope acquired. The raw data used for slope estimation is the measured stage of the free surface acquired at two observation points along the stream.

The illustration of the sensitivity analysis is applied to two gaging sites quite different in terms of hydraulic characteristics and instrumentation used for the raw data acquisition. The first site is Naju Bridge (South Korea) the same as the one described in Section 4.3. The second site is located on a small stream (Clear Creek in Iowa) in the proximity of the USGS gaging station # 05454220 near Oxford (Iowa, USA). This stream is relatively small (i.e., about 10-m wide (at base flow) with a bed slope of 0.0004. The data for the slope estimation is collected with a sampling rate of 10-min at the first site and 15-min at the second one for the largest storm of the year 2022.

Implementation of the smoothing procedures identified for the analysis of index velocity are used to assess the performance of the procedures when implemented to free-surface slope measurement using a simplified set of criteria for the performance matrix. The results of the evaluation for the Naju Bridge site are shown in Figure 15 while the same analysis for the Clear Creek site is shown in Figure 16.

The inspection of the results in Figure 15 reveals that GS, LR, FFS, and QR exhibit consistent linear trends much below the observed data values, similarly to the smoothed traces on the index-velocity data reported in Figure 14. A similar linear smoothing effect is obtained with the SG method by the magnitude of the values are closer to the raw data. While the approaches of DWT,

KS, and MA-based have demonstrated successful results, it can be argued that the optimal smoothing algorithm for the free-surface slope acquired at this site using the WHS technique.

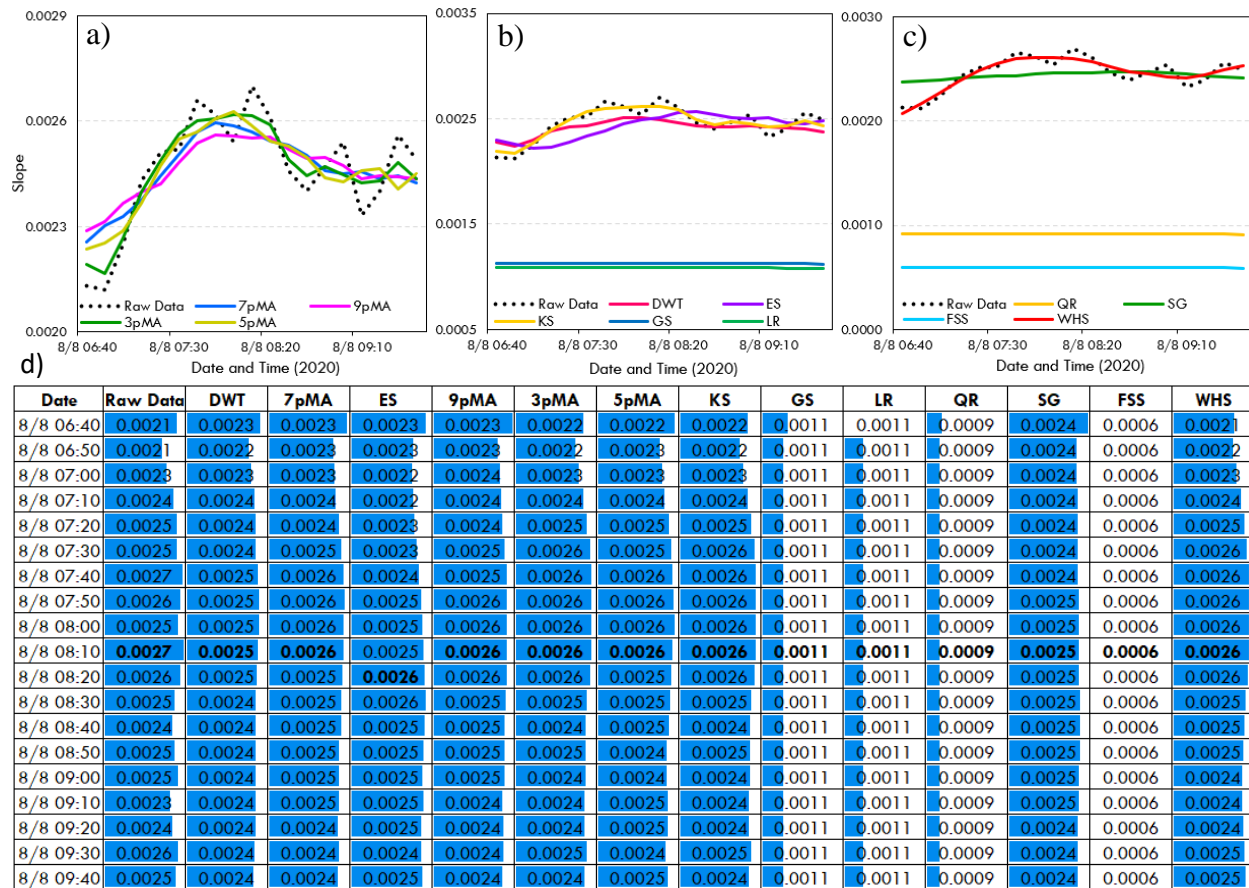


Figure 15. Smoothed data obtained with the selected methods applied to 10-min stage data for a selected storm event at the Naju Bridge gaging site (Korea): a) smoothed data with 3-5-7-9p MA; b) smoothed data with DWT, ES, KS, GS, and LR; c) QR, SG, FSS, and WHS; and d) the heat map of the smoothed datasets (the peak values for the storm as obtained with each smoothing procedure are printed in bold in the table).

Figure 16 displays distinct outcomes from those reported in Figures 14 and 15. Out of all tested MA-based methods, it seems that only the 5-p MA method closely approximates the trends indicated by the raw data, followed closely by the KS and DWT methods in terms of efficiency (see Figure 16b). Furthermore, GS, LR, QR, and GS methods are effective in smoothing the data, in contrast with their effect on the data displayed in Figure 14 and 15. The ES method displays a large time shift compared to all other methods (see Figure 16b). The FSS, SG, and WHS methods are closely together in Figure 16c, but the shift in magnitude is quite large. FSS may first appear to provide effective smoothing, it ultimately leads to the presence of several peaks in the data. The WHS dataset yielded outstanding outcomes, as did all datasets with less data (datasets containing less than 15-minute yearly data).

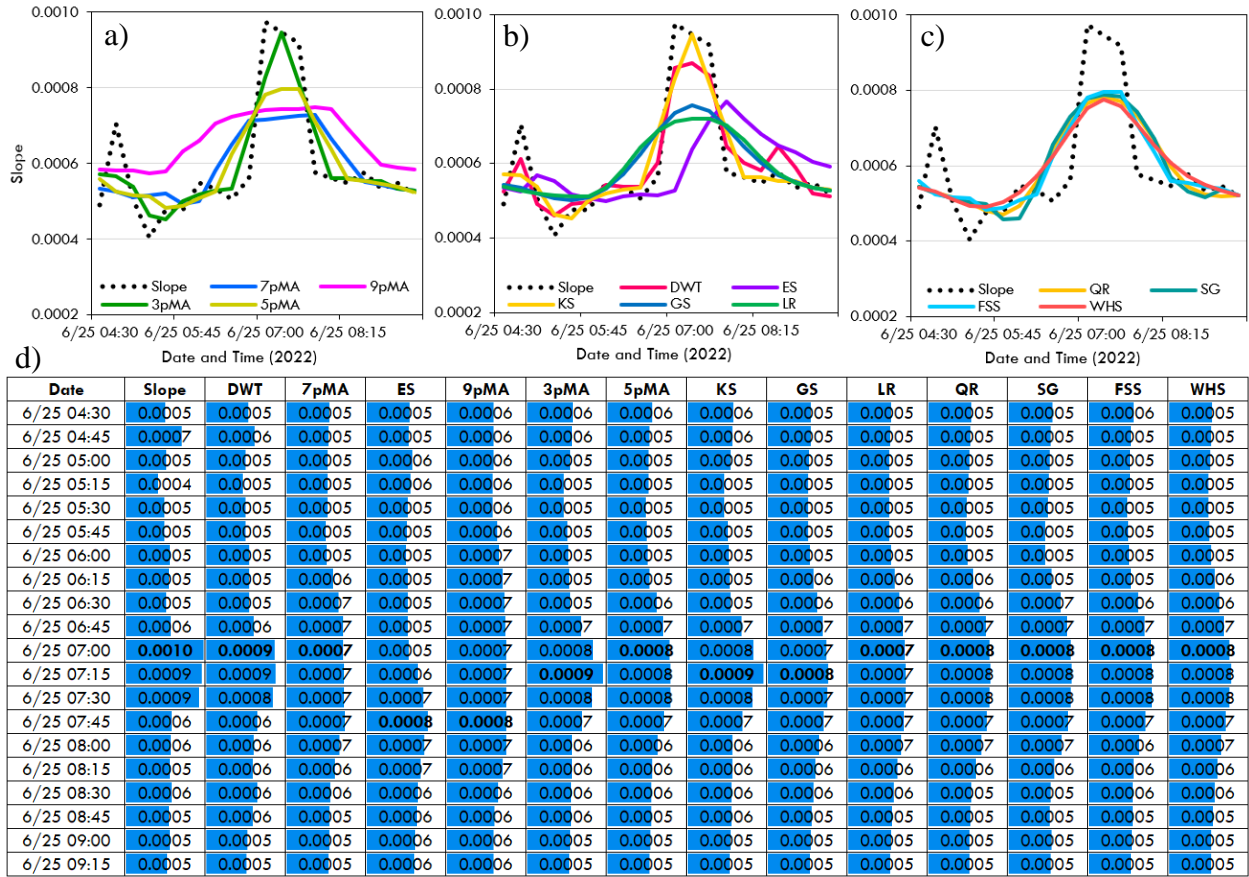


Figure 16. Smoothed data obtained with the selected methods applied to 15-min stage data for a storm event at the Clear Creek gaging site (USGS station # 05454220): a) smoothed data with 3-5-7-9p MA; b) smoothed data with DWT, ES, KS, GS, and LR, c) QR, SG, FSS, and WHS; d) the heat map of the smoothed datasets (the peak values for the storm as obtained with each smoothing procedure are printed in bold in the table).

5. Discussions

There are several persistent research questions relevant to the complex flow dynamics associated with flood wave propagation in channels. Clear resolutions to these questions continue to be challenging as the inferences from the analytical, experimental, and numerical investigations are limited (Hager et al., 2019). The primary source for robust information and actual data about these complex flow dynamics and processes can be obtained through direct measurements. However, this data could not be obtained with traditional monitoring techniques and has only recently become available due to advances in novel measurement techniques. The newly acquired data is massive and buried within inherent flow perturbations and observational noise making it difficult to answer critical questions on whether and how the changes in one variable cause changes in another. The present analysis was motivated by the need to filter the in-situ data for using them to

address qualitative domain knowledge and quantitatively answer these questions. The main goal of this analysis is to set a mathematical foundation for the empirical results that can lead to unified generalized conclusions on principles or laws for unsteady flows propagating in open channels and formulating practical guidance for future data acquisition and processing.

As can be noticed from the set of multivariate data presented in the analysis, the digital discrete data sampled at constant rates display nonlinearity and nonstationary and cannot be fully predicted by theory or numerical simulations as none can describe all possible fluctuations generated by larger or smaller flow pulses. The sources of these pulses are spatial and temporal changes in precipitation intensity or inflows from upstream tributaries and they cannot be fully captured by modeled as there is no data at sufficient resolutions to realistically inform on the changes in the disturbance source.

Moreover, the measurements for stream monitoring are obtained with multiple methods and instruments that bring in uncertainty of the natural environment, instrument accuracy and instrument operation. The streamflow measurements are inherently and notoriously noisy, with a cumulative probable uncertainty estimated in the 6% to 19% range (Harmel et al., 2006). This large range of uncertainty in measurements becomes a source of noise when attempting to decipher the details of the relationships among flow variables around the hydrograph peaks, with both the magnitude and timing being of critical importance. Moreover, the data uncertainty is commensurate with the signal magnitude, an additional complexity in uniformly applying the data conditioning protocols.

From the onset of the analysis, the key question was if the filtering or smoothing are the best data conditioning candidates for our type of time series. In general, filtering can be used when a subset or subrange of the data is preferentially selected to condition the time series. In our case the unwanted fluctuations and noise are not easily distinguished from the actual variabilities that must be preserved. The smoothing effort focused on capturing the important patterns in the data, while potentially leaving out the noise and other flow perturbations that are not reflective of the targeted process. There are also multiple challenges when implementing smoothing as these techniques rely on the reasonability of the assumptions and the selection of the tuning parameters associated with individual smoothing methods. An early decision for our analysis was to choose smoothing over filtering as the former allows a more controlled evaluation environment by using the visual inspections as a guide for extracting the information from the data.

Following the initial stages, we embarked on exploring and screening the available data smoothing methods tempered by the expert knowledge of the investigated processes. We identified a plethora of data analysis concepts and techniques, both simpler as well as more complex, that are available for the hydrologic and hydraulic engineering context. A recurring theme has been whether a simple, or a more complex technique should be considered for the analysis. Complex statistical analyses can lead to incorrect inferences if the underlying model assumptions are incorrect (Muste et al., 2017). The published work on hydrometric lack specific guidance that address the processing methodological questions related to time series acquired in situ. Consequently, we selected the most often-used smoothing methods in the hydrologic and hydraulic

domain and rigorously tested these methods with a comprehensive set of statistical fitness parameters and generic ideas of the expected trends in the variation of the raw data. The joint inferences from the statistical fitness parameters complemented by the visual inspections are integral parts of a new screening process that led to the selection of the optimal data conditioning candidates for our investigation purposes.

The original screening process described in this study narrows the selection choices using a flexible but robust workflow. It does so by acting at two levels, that can be envisioned as the workflow dimensions. The first dimension enables the tuning of the fitness parameters for each of the smoothing methods until the outcomes match the trends prescribed by the theoretical formulations or the sparse experimental evidence (Muste et al., 2024). The second dimension progressively eliminates the methods based on the expert understanding of the relevance of the numerical and visual inspections. The two-dimensional screening steps are not rigid; they can be interchanged, reduced, or enhanced according to the quality of the outcomes observed for each step in the progression. The efficiency of the screening process is demonstrated by the difference in the selection outcomes when implemented with different input datasets, i.e., 15-min vs. 1-hr sampling frequency for the same variable (see Figure 4).

The sensitivity study applied to several measurement scenarios substantiated that the same method applied to different peak hydrograph shapes performed slightly differently. Similarly, the length of the time span for the data subject to smoothing can produce slightly different results. These manifestations are expected due to the nonlinearity of the data and the iterative characteristics inherent in the employed smoothing methods. Fortunately, the screening protocol proposed in the study allows for gradual parameter adjustments when the outcome of a smoothing method does not fulfill the expected trends in the raw data. A possible remediation of the above limitations (suggested for future research) is the sub-setting of the storm types based of a generic set of parameters and application of the smoothing methods for specific type of storms.

The proposed screening framework is intended as a starting point and the users are encouraged to delve further into literature to become aware of the statistical bases for each methodology and the subtleties of the analysis. With the increase of the experience with the screening workflow, the gap between the statistical and domain science narrows enabling the implementation of the process through machine learning techniques rather than user intervention.

6. Conclusion

The nonstationary and noisy structure of the data acquired in natural streams poses significant obstacles in understanding and formulating theoretical foundations for complex processes occurring during highly unsteady flow events. A clear understanding of these processes is needed to effectively support numerical and data-driven models used for forecasting purposes. The study introduces a screening protocol aimed at conditioning flow variables acquired under different conditions using adaptive and rigorous statistical measures informed by a broad understanding of the physical phenomena involved in the propagation of flood waves. The screening protocol is

designed to select data smoothing methods that discern trends among interconnected variables with the focus on their relationship at the peak of the hydrographs.

One key objective of the smoothing protocol is to filter out noise and fluctuations while carefully preserving the key temporal gradients and trends needed to represent the complexity of the flow dynamics. The usefulness of the newly developed protocol was tested with a set of 18 smoothing methods applied to 6 datasets distinguished by the nature of the measured time series (index-velocity and free surface slope), measurements sampling rates (every 10-min, 15-min, and 1-hr) and influence of the measurement site (3 locations). A total of 118 datasets were analyzed by changing parameters of the smoothing procedures and testing their sensitivity at the above-mentioned factors. The results of the screening protocol implementation led to some preliminary conclusions on the efficiency of the data smoothing algorithms when applied to measurements of flow variables. We are aware that the performance assessment is not exhaustive as we analyzed a limited number of smoothing procedures and datasets. However, the samples used for illustrations are statistically and physically significant to point to the issues that are to be considered when employing smoothing.

A broad assessment of the capability of the smoothing protocols to detect the magnitude and timing of the peak hydrograph across all tests indicates the following categories:

Highly efficient: 3-p, 5-p, 7-p, and 9-p MA-based methods. The 3-p MA and 5-p MA hold a prominent position that is beneficial method were optimal that is also optimal as they are processing data in a narrow time window. Although the discrete wavelet transform (DWT) outperforms moving averages (MAs) when applied to all data, its performance is only slightly inferior to MAs when applied specifically to storms. It may be asserted that DWT has superior performance when evaluated with larger datasets. KS is also listed in this category but with slightly lower performance. The WHS method performs also well when the tested with smaller datasets.

- Medium efficient: 3pWMA, ES, SG, 3pEMA, EMD, and HHT methods.
- Modest to low efficient: FSS, LOWESS, GS, LR, and QR methods.

The above inferences demonstrate that, in certain cases, employing basic techniques such as moving average approaches (the least sophisticated smoothing tools in the pool of candidates) can yield highly effective smoothing outcomes, whereas more intricate methods with more computational demands may produce inferior results. As deceptive as this finding might be, there is a need for thorough evaluations to reach this conclusion.

Acknowledgement

The authors acknowledge the partial support offered by the NSF EAR-HS 2139649 award that triggered the need for this study. The fourth author acknowledges the support of the NA22NWS4320003 award funded by NWS/NOAA. Special thanks to Ciprian Bacotiu (Technical University Cluj-Napoca, Romania) and Fleit Gabor (Budapest University of Technology and Economics, Budapest, Hungary) for their comments that enriched the discussions regarding this analysis.

Data Availability:

The data used in this study is available upon request.

References:

- Bae, I., & Ji, U. (2019). Outlier detection and smoothing process for water level data measured by ultrasonic sensor in stream flows. *Water*, *11*(5), 951. <https://doi.org/10.3390/w11050951>
- Baydaroglu, Ö., Koçak, K., & Duran, K. (2017). River flow prediction using hybrid models of support vector regression with the wavelet transform, singular spectrum analysis and chaotic approach. *Meteorology and Atmospheric Physics*, *130*(3), 349-359. <https://doi.org/10.1007/s00703-017-0518-9>
- Baydaroglu, Ö., & Demir, I. (2023). Temporal and Spatial Satellite Data Augmentation for Deep Learning-Based Rainfall Nowcasting. <https://doi.org/10.31223/X5QQ39>
- Cleveland, W. S. (1979). Robust locally weighted regression and smoothing Scatterplots. *Journal of the American Statistical Association*, *74*(368), 829-836. <https://doi.org/10.1080/01621459.1979.10481038>
- Cleveland, W. S., & Devlin, S. J. (1988). Locally weighted regression: An approach to regression analysis by local Fitting. *Journal of the American Statistical Association*, *83*(403), 596-610. <https://doi.org/10.1080/01621459.1988.10478639>
- Daubechies, I. (1988). Orthonormal bases of compactly supported wavelets. *Communications on Pure and Applied Mathematics*, *41*(7), 909-996. <https://doi.org/10.1002/cpa.3160410705>
- Demir, I., Conover, H., Krajewski, W.F., Seo, B.C., Goska, R., He, Y., McEniry, M.F., Graves, S.J. and Petersen, W., (2015). Data-enabled field experiment planning, management, and research using cyberinfrastructure. *Journal of Hydrometeorology*, *16*(3), pp.1155-1170.
- Demir, I., & Szczepanek, R. (2017). Optimization of river network representation data models for web-based systems. *Earth and Space Science*, *4*(6), 336-347.
- Friedman, J. H. (1984). A variable span smoother. Stanford Univ CA lab for computational statistics. <https://doi.org/10.21236/ada148241>
- Hager, W. H., Castro-Orgaz, O., & Hutter, K. (2019). Correspondence between de Saint-Venant and Boussinesq. 1: Birth of the shallow-water equations. *Comptes Rendus Mécanique*, *347*(9), 632-662. <https://doi.org/10.1016/j.crme.2019.08.004>
- Hannachi, A. (2021). Patterns identification and data mining in weather and climate. *Springer Atmospheric Sciences*. <https://doi.org/10.1007/978-3-030-67073-3>
- Harmel, R. D., Cooper, R. J., Slade, R. M., Haney, R. L., & Arnold, J. G. (2006). Cumulative uncertainty in measured streamflow and water quality data for small watersheds. *Transactions of the ASABE*, *49*(3), 689-701. <https://doi.org/10.13031/2013.20488>
- Henderson, R. (1924). A new method of graduation. *Transactions of the Actuarial Society of America*, *25*, 29-40.
- Henderson, R. (1925). Further remarks on graduation. *Transactions of the Actuarial Society of America*, *26*, 52-57.

- Holt, C. C. (2004a). Forecasting seasonals and trends by exponentially weighted moving averages. *International Journal of Forecasting*, 20(1), 5-10. <https://doi.org/10.1016/j.ijforecast.2003.09.015>
- Holt, C. C. (2004b). Author's retrospective on 'Forecasting seasonals and trends by exponentially weighted moving averages'. *International Journal of Forecasting*, 20(1), 11-13. <https://doi.org/10.1016/j.ijforecast.2003.09.017>
- Huang, N. E., Long, S. R., & Shen, Z. (1996). The mechanism for frequency Downshift in nonlinear wave evolution. *Advances in Applied Mechanics*, 59-117C. [https://doi.org/10.1016/s0065-2156\(08\)70076-0](https://doi.org/10.1016/s0065-2156(08)70076-0)
- Huang, N. E., Shen, Z., Long, S. R., Wu, M. C., Shih, H. H., Zheng, Q., Yen, N., Tung, C. C., & Liu, H. H. (1998). The empirical mode decomposition and the Hilbert spectrum for nonlinear and non-stationary time series analysis. *Proceedings of the Royal Society of London. Series A: Mathematical, Physical and Engineering Sciences*, 454(1971), 903-995. <https://doi.org/10.1098/rspa.1998.0193>
- Huang, N. E., Shen, Z., & Long, S. R. (1999). A new view of nonlinear water waves: The Hilbert spectrum. *Annual Review of Fluid Mechanics*, 31(1), 417-457. <https://doi.org/10.1146/annurev.fluid.31.1.417>
- Huang, N. E., Wu, M. C., Long, S. R., Shen, S. S., Qu, W., Gloersen, P., & Fan, K. L. (2003). A confidence limit for the empirical mode decomposition and Hilbert spectral analysis. *Proceedings of the Royal Society of London. Series A: Mathematical, Physical and Engineering Sciences*, 459(2037), 2317-2345. <https://doi.org/10.1098/rspa.2003.1123>
- Findikakis, A.N. and Savic, D. (2021). Artificial Intelligence, Editorial in Hydrolink Magazine, 2, 2021, International Association of Hydro-Environment and Research, Madrid, Spain.
- Karlöf, L., Ølgård, T., Godtliebsen, F., Kaczmarska, M., & Fischer, H. (2005). Statistical techniques to select detection thresholds for peak signals in ice-core data. *Journal of Glaciology*, 51(175), 655-662. <https://doi.org/10.3189/172756505781829115>
- Kowalski, P., & Smyk, R. (2018). Review and comparison of smoothing algorithms for one-dimensional data noise reduction. *2018 International Interdisciplinary PhD Workshop (IIPhDW)* (pp. 277-281). IEEE. <https://doi.org/10.1109/iiphdw.2018.8388373>
- Krajewski, W. F., Ghimire, G. R., Demir, I., & Mantilla, R. (2021). Real-time streamflow forecasting: AI vs. Hydrologic insights. *Journal of Hydrology X*, 13, 100110.
- Levesque, V. A., & Oberg, K. A. (2012). *Computing discharge using the index velocity method* (pp. 3-A23). Reston, VA, USA: US Department of the Interior, US Geological Survey. <https://doi.org/10.3133/tm3a23>
- Li, Z., & Demir, I. (2022). A comprehensive web-based system for flood inundation map generation and comparative analysis based on height above nearest drainage. *Science of The Total Environment*, 828, 154420.
- Ligue, K.B.D. and Acosta, J.E. (2021). Smoothing river discharge time series computed using the velocity-area method.

- Maity, R. (2018). Theory of copula in hydrology and Hydroclimatology. *Statistical Methods in Hydrology and Hydroclimatology*, 381-424. https://doi.org/10.1007/978-981-10-8779-0_10
- Mallat, S. (1989). A theory for multiresolution signal decomposition: The wavelet representation. *IEEE Transactions on Pattern Analysis and Machine Intelligence*, 11(7), 674-693. <https://doi.org/10.1109/34.192463>
- McLaughlin, D. (2002). An integrated approach to hydrologic data assimilation: Interpolation, smoothing, and filtering. *Advances in Water Resources*, 25(8-12), 1275-1286. [https://doi.org/10.1016/s0309-1708\(02\)00055-6](https://doi.org/10.1016/s0309-1708(02)00055-6)
- Mrokowska, M. M., Rowiński, P. M., & Kalinowska, M. B. (2013). The uncertainty of measurements in river hydraulics: Evaluation of friction velocity based on an unrepeatable experiment. *GeoPlanet: Earth and Planetary Sciences*, 195-206. https://doi.org/10.1007/978-3-642-30209-1_13
- Muste, M., Lyn, D.A., Admiraal, D., Eterna, R., Nikora, V., & Garcia, M.H. (Eds.). (2017). Experimental hydraulics: Methods, instrumentation, data processing and management: Volume I: Fundamentals and methods. CRC Press.
- Muste, M., Bacotiu, C., & Thomas, D. (2019, September). Evaluation of the slope-area method for continuous streamflow monitoring, In Proceedings of the 38th IAHR World Congress, (pp. 121-130).
- Muste, M., Lee, K., Kim, D., Bacotiu, C., Oliveros, M. R., Cheng, Z., & Quintero, F. (2020). Revisiting hysteresis of flow variables in monitoring unsteady streamflows. *Journal of Hydraulic Research*, 58(6), 867-887. <https://doi.org/10.1080/00221686.2020.1786742>
- Muste, M., Kim, D., & Kim, K. (2022a). A flood-crest forecast prototype for river floods using only in-stream measurements. *Communications Earth & Environment*, 3(1). <https://doi.org/10.1038/s43247-022-00402-z>
- Muste, M., Kim, D., & Kim, K. (2022b). Insights into flood wave propagation in natural streams as captured with acoustic profilers at an index-velocity gaging station. *Water*, 14(9), 1380. <https://doi.org/10.3390/w14091380>
- Muste, M., Kim, K., Kim, D. and Fleit G. (2024). Decoding the hysteretic behavior of hydraulic variables in lowland rivers with multivariate monitoring methods, *Hydrological Processes* (under review, 2024)
- Nadaraya, E. A. (1964). On estimating regression. *Theory of Probability & Its Applications*, 9(1), 141-142. <https://doi.org/10.1137/1109020>
- Nazir, H. M., Hussain, I., Ahmad, I., Faisal, M., & Almanjahie, I. M. (2019). An improved framework to predict river flow time series data. *PeerJ*, 7, e7183. <https://doi.org/10.7717/peerj.7183>
- Prowse, C. W. (1984). *Some thoughts on lag and hysteresis*. *Area*, 16(1), 17-23.
- Rantz, S. E. (1982). *Measurement and computation of streamflow (Vol. 2175)*. US Department of the Interior, Geological Survey.

- Runge, J., Gerhardus, A., Varando, G., Eyring, V., & Camps-Valls, G. (2023). Causal inference for time series. *Nature Review Earth & Environment* 4(7), 487–505. <https://doi.org/10.1038/s43017-023-00431-y>
- Savitzky, A., & Golay, M. J. (1964). Smoothing and differentiation of data by simplified least squares procedures. *Analytical Chemistry*, 36(8), 1627-1639. <https://doi.org/10.1021/ac60214a047>
- Sit, M., Demiray, B., & Demir, I. (2021). Short-term hourly streamflow prediction with graph convolutional GRU networks. arXiv preprint arXiv:2107.07039.
- Smith, C. F., Cordova, J. T., & Wiele, S. M. (2010). *The continuous slope-area method for computing event hydrographs*. U. S. Geological Survey. <https://doi.org/10.3133/sir20105241>
- Swarup, S., Braverman, V., Arora, R., Caragea, D., Cragin, M., Dy, J., ... & Yang, C. (2018, June). Challenges and opportunities in big data research: Outcomes from the second annual joint PI meeting of the NSF BIGDATA research program and the NSF big data regional innovation hubs and spokes programs 2018. *In NSF Workshop Reports*.
- Wang, H. W., Lin, G. F., Tfwala, S. S., & Hong, J. H. (2019). Filtering continuous river surface velocity radar data. *Water*, 11(4), 764. <https://doi.org/10.3390/w11040764>
- Watson, G. S. (1964). Smooth regression analysis. *Sankhyā: The Indian Journal of Statistics, Series A*, 359-372.
- Whittaker, E. T. (1922). On a new method of graduation. *Proceedings of the Edinburgh Mathematical Society*, 41, 63-75. <https://doi.org/10.1017/s0013091500077853>
- Whittaker, E. T. (1925). VIII.—On the theory of graduation. *Proceedings of the Royal Society of Edinburgh*, 44, 77-83. <https://doi.org/10.1017/s0370164600020800>
- WMO. (2010). Manual on stream gauging, volume 1—fieldwork. World Meteorological Organization.